Isotactic Polypropylene Microfiber Prepared by Carbon Dioxide Laser-Heating

Akihiro Suzuki, Shinichi Narusue

Interdisciplinary Graduate of School of Medicine and Engineering, University of Yamanashi, Takeda-4, Kofu 400-8511, Japan

Received 9 May 2003; accepted 30 October 2003

ABSTRACT: An isotactic polypropylene (i-PP) microfiber was obtained by irradiating a carbon dioxide laser to previously drawn fibers. To prepare the thinner i-PP microfiber, it is necessary to previously draw original i-PP fibers under an applied tension of 7.8 MPa at a drawing temperature of 140°C. The drawn fiber was heated under an applied tension of 0.3 MPa using the laser operated at a power density of 39.6 W cm^{-2}. The thinnest i-PP microfiber obtained under optimum conditions had a diameter of 1.8 μm and a birefringence of 30×10^{-3}. Its draw ratio estimated from the diameter reached 51,630. It is so far impossible to achieve such a high draw ratio by any drawing. The wide-angle X-ray diffraction photograph of the microfiber shows the existence of the oriented crystallites. Laser-heating allows easier fabrication of microfibers compared with the conventional technology such as the conjugate spinning. © 2004 Wiley Periodicals, Inc. J Appl Polym Sci 92: 1534–1539, 2004

Key words: isotactic polypropylene (i-PP); fibers; drawing; differential scanning calorimetry (DSC); birefringence

INTRODUCTION

A carbon dioxide (CO_2) laser has been applied to welding, cutting, and cladding for ceramics and metals, annealing of semiconductors, improvement of the surface properties of carbon or other ceramic fibers, etching of polymer, and curing of epoxy resin.[1–8] We applied a continuous-wave carbon dioxide (CW CO_2) laser to poly(ethylene terephthalate) (PET)[9] and nylon 6[10] fibers to improve their mechanical properties. The drawing and annealing by using the CW CO_2 laser was found to be effective in producing fibers with high modulus and high strength.

In preliminary experiments to optimize a laser-heating zone-drawing condition for the PET fibers it was unexpectedly found that PET microfibers were prepared by irradiating the laser at a higher power under application of very low tension when compared with the laser-heating zone-drawing.[11] The one-step thinning by laser heating gave a PET microfiber having a diameter of 4.6 μm and birefringence of 0.112. Furthermore, it was found that the thinner PET microfiber was easily obtained by irradiating the high-output power laser to the PET fiber previously drawn and annealed (two-step thinning).[12] The PET microfiber obtained by two-step thinning had a diameter of 1.5 μm and birefringence of 0.173. The two-step thinning of nylon 6 fiber also gave the microfiber with a diameter of 1.9 μm and a birefringence of 46.2×10^{-3}.[13] Its draw ratio estimated from the diameter reached 9895.

Microfibers are now manufactured with an especially highly skilled technique such as conjugate spinning, which requires a highly complex spinneret, and it is impossible to prepare microfibers by drawing methods. However, we found that laser heating easily produces PET and nylon 6 microfibers without the use of highly skilled techniques.

In this study, the two-step thinning method was applied to an isotactic polypropylene (i-PP) fiber to prepare a thinner i-PP microfiber. We present here the results pertaining to the properties of the i-PP microfiber obtained by the CW CO_2 laser heating.

EXPERIMENTAL

Materials

An original i-PP fiber was produced from commercial-grade i-PP pellets by using a laboratory-scale melt extruder and takeup unit. Its tacticity was highly isotactic (~ 96%), which was determined by using nuclear magnetic resonance techniques. The original fibers were spun into monofilaments at a spinning temperature of 230°C. The original fibers had a diameter of 409 μm, degree of crystallinity of 44%, and birefringence of 0.3×10^{-3}.

Correspondence to: A. Suzuki (a-suzuki@yamanashi.ac.jp).
Contract grant sponsor: Japan Society for the Promotion of Science.

Measurements

The birefringence was measured with a polarizing microscope equipped with a Berek compensator (Olympus Optical Co., Osaka, Japan).

Density (ρ) was measured at 23°C by a flotation technique using a carbon tetrachloride and toluene mixture. The degree of crystallinity, expressed as a weight fraction (X_w), was obtained using the relation

$$X_w = \frac{\rho_c(\rho - \rho_a)}{\rho(\rho_c - \rho_a)} \times 100 \quad (1)$$

where ρ_c and ρ_a are the densities of crystalline and amorphous phases, taken to be 0.936 and 0.850 g/cm^3, respectively.[14,15] The density of amorphous polymer was assumed to be constant, independent of treatments. However, the density of the microfiber could not be measured by the flotation technique because the specimen was very small.

The draw ratio can be calculated easily using the following equation:

$$\text{Draw ratio} = (d_0/d)^2 \quad (2)$$

where d_0 is the diameter of the original fiber and d is that of the microfiber, and the volumes before and after the thinning are assumed to be constant.

SEM micrographs of the fibers were observed on a JEOL JSM-T20 apparatus (JEOL, Tokyo, Japan) with an acceleration voltage of 19 kV.

Wide-angle X-ray diffraction photographs of the fibers were taken using a flat-film camera. The camera was attached to a Rigaku X-ray generator (Rigaku Co., Japan) that was operated at 36 kV and 18 mA. The radiation used was Ni-filtered Cu–K_α. The sample-to-film distance was 40 mm. The fiber was exposed for 4 h to the X-ray beam from a pinhole collimator with a diameter of 0.4 mm.

Differential scanning calorimetry (DSC) measurements were carried out using a Rigaku DSC 8230C calorimeter. The DSC scans were performed within the temperature range of 25 to 200°C, using a heating rate of 10°C/min. All DSC experiments were carried out under a nitrogen purge. The DSC instrument was calibrated with indium.

Apparatus for zone drawing

The zone drawing as a pretreatment of the laser thinning was carried out by using an apparatus similar to that described in detail elsewhere.[16] The zone-drawing apparatus consisted of a temperature-controlled zone heater and a Linead motor (Oriental Motor Co., Japan) capable of moving the zone heater at an arbitrary speed to locally heat the fiber. One end of the fiber was connected to a fixed support, whereas the other was connected to a weight after passing through a pulley. The zone drawing was carried out by moving the zone heater at a speed of 50 mm/min along the fiber axis under optimum tension.

TABLE I
Optimum Conditions for Two-Step Thinning and One-Step Thinning

Treatment	Applied tension (MPa)	Drawing temperature (°C)	Laser power density (W cm^{-2})
Two steps			
Zone-drawing	7.8	140	—
Laser-heating	0.3	—	39.6
One step			
Laser-heating	0.02	—	31.6

Laser-heating method

The CW CO_2 laser-heating apparatus used for producing the microfiber consisted of a CW CO_2 laser emitter (PIN10S, Onizca Glass Ltd., Japan), a power meter (Nova, Ophir Optronics Ltd., Wilmington, MA) with a thermal head, and an electric slider (LimoTM Oriental Motor Co., Japan). The electric slider was used to move the fiber at a constant speed. The CW CO_2 laser emitted light at 10.6 μm, and the laser beam was a 4.0 mm diameter spot. The laser power of more than 90% was obtained in the area of the 4.0-mm ϕ laser spot. The power density (PD) was estimated by dividing the measured laser power in the area of the laser spot. One end of the fiber was connected to a jaw equipped with the electric slider, whereas the other was attached to an arbitrary weight. The fiber was moved downward at a speed of 500 mm/min using the electric slider, and the laser beam was irradiated to the fiber. The fiber was instantly drawn by irradiating the CW CO_2 laser to the fiber moving at constant speed, after which the microfiber (length $\sim$ 1.5 m) was obtained.

RESULTS AND DISCUSSION

Thinning condition and properties of microfiber

The preparatory experiment was carried out to determine the optimum zone-drawing and laser-heating (two-step thinning) conditions to obtain a thinner i-PP microfiber. The optimum conditions for the zone drawing and laser heating were the conditions under which the highest birefringence in each treatment was obtained (given in Table I; that of one-step thinning was added to Table I to compare with the two-step thinning). The diameter, birefringence, and draw ratio for the fiber obtained by each optimum condition are given in Table II. A zone-drawn (ZD) fiber has a diameter of 131 μm, birefringence of 34 $\times$ 10^{-3}, and

TABLE II
Diameter, Birefringence, and Draw Ratio Estimated from Diameter for Original, Zone-Drawn (ZD), Zone-Drawn and Laser-Heated (ZD-LH) Fiber, and Laser-Heated (LH) Fiber

Fiber	Diameter (μm)	Birefringence ($\times 10^3$)	Draw ratio
Original fiber	409	0.3	—
Two steps			
ZD fiber	131	34	9.7
ZD-LH fiber	1.8	30	51,630
One step			
LH fiber	7.6	18	2,883

draw ratio of 9.7. The fiber obtained by laser heating the ZD fiber [i.e., a zone-drawn and laser-heated (ZD-LH) fiber] has a diameter of 1.8 μm and birefringence of 30×10^{-3}. The draw ratio of the ZD-LH fiber reached 51,630. It is so far impossible to achieve such a high draw ratio by any drawing method. The birefringence of the ZD-LH fiber was approximately equal to the birefringence of an intrinsic crystallite (33.1×10^{-3}).[17] On the other hand, the fiber obtained by one-step thinning [i.e., a laser-heated (LH) fiber] has a diameter of 7.6, birefringence of 18×10^{-3}, and draw ratio of 2883.

Figure 1 shows the SEM micrographs for the original and the ZD-LH fiber. The SEM observation at a magnification of $\times$5000 shows that the ZD-LH fiber has a smooth surface (without a surface roughened by laser ablation) and is uniform in diameter.

Neck prepared by laser heating

Figure 2 shows microphotographs of the upper and lower spindle-shaped necks in the ZD-LH fiber. The two spindle-shaped necks are formed at both ends of the ZD-LH fiber (length $\sim$ 1.5 m). The formation of the spindle-shaped neck suggests that the ZD fiber, heated locally by irradiating the laser, melted instantly. To elucidate the formation process of the spindle-shaped neck, the change of shape of the fiber irradiated by the laser with time was observed by a microscope. Figure 3 shows the microphotographs of the laser-heated fiber after 0.35, 0.40, and 0.80 s from laser irradiation. The laser-irradiated part is expanded, constricted in the middle, and formed the spindle-shaped neck.

A series of these processes in the formation of the spindle-shaped neck is thought to explain the thinning mechanism as follows. The temperature of the i-PP fiber heated by the laser instantly reaches a high temperature that exceeds its melting temperature. The

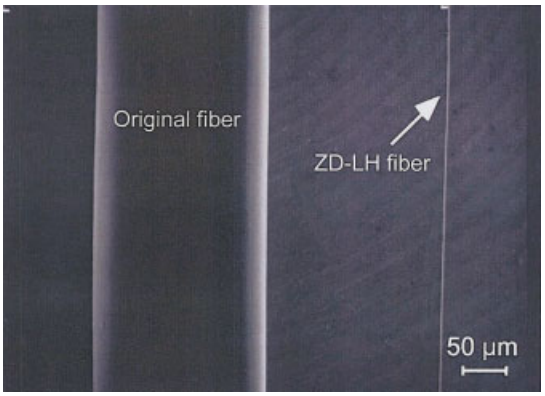

Figure 1 SEM micrographs of the original and the ZD-LH fiber.

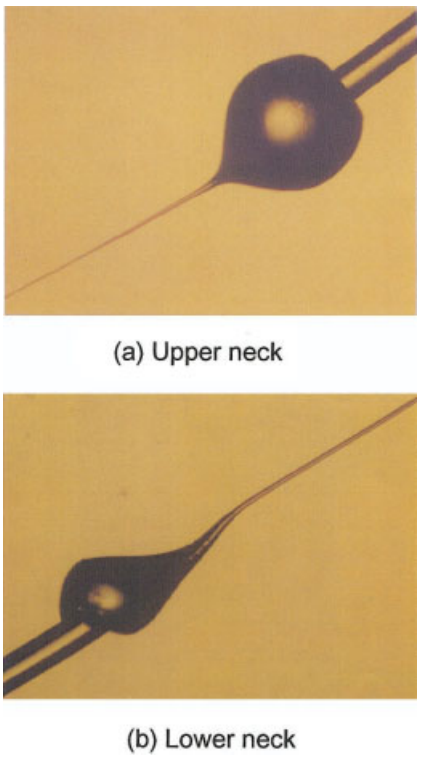

Figure 2 Microphotographs of the upper and lower spindle-shaped necks in the ZD-LH fiber.

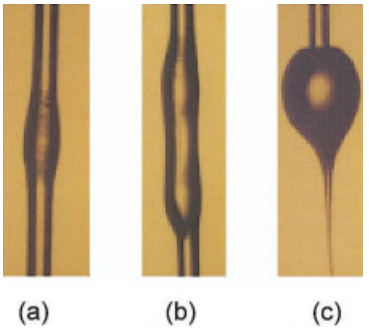

Figure 3 Microphotographs of the laser-heated fiber after (a) 0.35, (b) 0.40, and (c) 0.80 s from laser irradiation.

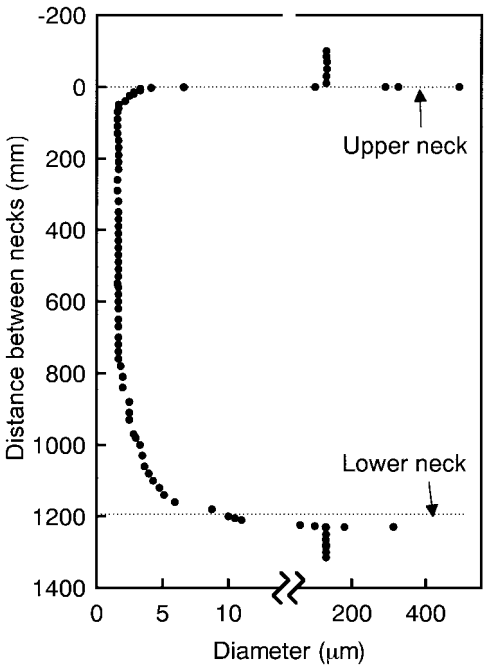

Figure 4 Changes in the diameter along fiber axis for the ZD-LH fiber.

melt viscosity in the part of the heated ZD fiber becomes sufficiently low without elongation or cutting because the applied tension during the laser heating is sufficiently lower than that during the laser heating zone drawing. Then the heated part is rendered to an instantaneous molten state. The microfiber was prepared by spinning from an instantaneous molten state, as is clear from the microphotograph of the spindle-shaped neck as shown in Figures 1 and 2. As a result of the laser heating under extremely low applied tension at high-output power, the plastic flow occurs at a high strain rate after the melt viscosity became sufficiently low. However, the instantaneous plastic flow induces the molecular orientation and crystallization in spite of a large deformation, just like in flow drawing, and gives an oriented i-PP microfiber. Thinning by use of the CW CO_2 laser may be considered as a dieless spinning.

Changes in diameter and birefringence along fiber axis

Figures 4 and 5 show the changes in the diameter and birefringence along the fiber axis for the ZD-LH fiber. The diameter and birefringence were measured at intervals of 20 mm along the fiber axis. The diameter is uniform except for the diameters in areas near the upper and lower necks. The spindle-shaped necks are characterized by almost optical isotropy because the birefringence in the necks is about 5×10^{-3}. The optical isotropy in the necks shows that the fiber irradiated by the laser was once locally molten. Although there is some scattering in the birefringence, the measurements of the birefringence along the fiber axis are about 30×10^{-3} and gradually decrease as it approaches the lower neck.

Wide-angle X-ray diffraction of the microfiber

Figure 6 shows the wide-angle X-ray diffraction photographs of the original, ZD, ZD-LH, and LH fibers. The ZD fiber has three strong equatorial reflections {(110), (040), and (130)} and two weak reflections {(060) and (220)}. The ZD-LH fiber has three strong equatorial reflections, but does not show two weak reflections. The LH fiber shows indistinct reflections on the equator, and a slight diffraction is observed. The ZD-LH fiber is inferior to the ZD fiber in degree of crystallinity and orientation, but is excellent compared to the LH fiber. Two-step thinning further improved the degree of crystallinity and orientation compared with one-step thinning. These results suggest that the strain-induced crystallization occurs by an instantaneous large deformation in spite of the flow drawing from the molten state, in the two-step thinning.

The i-PP crystallizes in three polymorphic forms: α-monoclinic, β-hexagonal,[18–20] and γ-orthorhombic crystal forms.[21,22] The α-form is the most stable crystalline phase and can be easily obtained by crystallization from the melt or from solution.[23] The α-form is further classified into two limiting modifications, that is α_1 and α_2.[24,25] The α_1-form is characterized by a

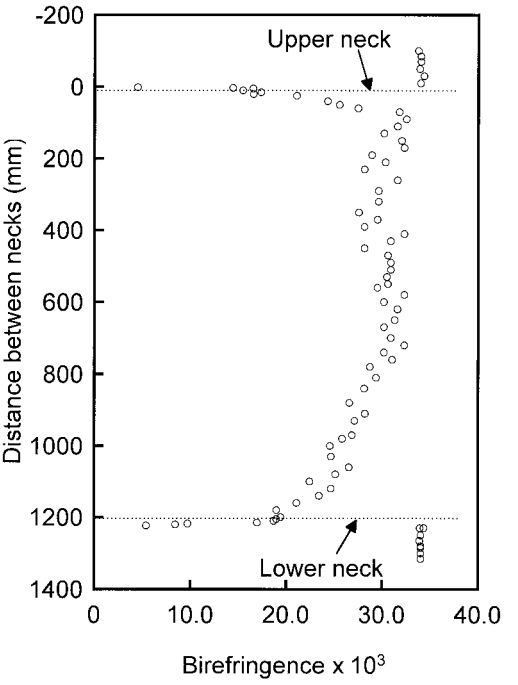

Figure 5 Changes in birefringence along fiber axis for the ZD-LH fiber.

Figure 6 Wide-angle X-ray diffraction photographs of the original, ZD, ZD-LH, and LH fibers.

statistical disorder like that described for the space group C2/c. The α_2-form is characterized by regularity of up and down positioning of the chains, as in the space group P21/c.

Both the α_1- and α_2-forms have substantially identical X-ray spectra. However, whereas only reflections with (h + k) even are allowed in the α_1-form, reflections with (h + k) odd may be present in the α_2-form.[26] All reflections observed are reflections with (h + k) even. It is known that the β-form exhibits a strong equatorial reflection (300) at $2\theta = 16.10°$, and that the γ-form[27] is observed (113) at $2\theta = 14.98°$ and (117) at 20.06°. However, no reflections attributed to the β-form and γ-form are observed in Figure 5. Therefore, these wide-angle X-ray diffraction photographs show that only the α_1-form exists in the ZD and the ZD-LH fibers.

Melting behavior of the microfiber

Figure 7 shows DSC curves of the original, the ZD, and ZD-LH fibers. The DSC curves show the presence of only one peak. The original fiber has a single melting endotherm peak at 161°C, and the ZD fiber has the sharper single melting endotherm peak at 167°C. A sharpening of the melting peak with zone drawing is caused by an increase in the degree of perfection of the crystallites.[28,29] The ZD-LH fiber has a broad melting endotherm peak at 166°C.

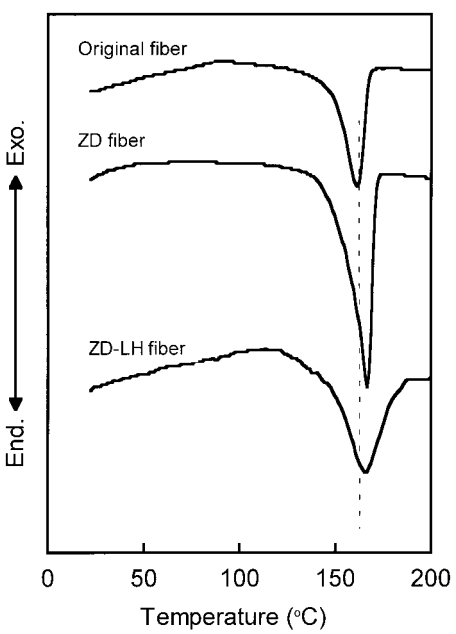

Figure 7 DSC curves of the original, the ZD, and ZD-LH fibers.

The difference in the melting temperature between the original and the ZD fibers has a substantial influence on the diameter of the obtained microfibers. The increase of the melting temperature makes it possible to irradiate the higher-output laser to the fiber. The higher the laser power, the lower the local melt viscosity in the irradiated fiber. The lower melt viscosity induces a large deformation at a faster strain rate. The instantaneous large deformation induced by the higher-output laser causes the stain-induced crystallization and produces a thinner microfiber.

Although the position of the melting peak for the ZD-LH fiber scarcely changes, its shape becomes wide when compared with that for the ZD fiber. The broadening of the melting peak is attributable to a disproportionation in the degree of perfection of the crystallites. These melting peaks show that the ZD-LH fiber is inferior to the ZD fiber in the uniformity of the crystallites.

The melting behavior of i-PP crystallized in different ways was previously studied by several investigators.[30–36] An endotherm peaking at 161°C is attributed to the melting of the α_1-form, and the high endotherm peaking above 170°C is attributed to the melting of the α_2-form.[33] Jacoby et al.[25] reported that the melting endotherm attributed to melting of the β-form was observed at about 150°C. No β-form was detected in the wide-angle X-ray diffraction photographs, as shown in Figure 6. The melting peaks in Figure 7 are located in the temperature range of 160 to 167°C, which means, therefore, that all melting peaks are attributed to the melting of the α_1-form. These results were substantiated by the wide-angle X-ray diffraction photographs.

CONCLUSIONS

It was determined that the two-step thinning technique, composed of zone drawing and CW CO_2 laser

heating, is capable of producing the i-PP microfiber. The zone drawing was carried out at a drawing temperature of 140°C under an applied tension of 7.8 MPa, and the zone-drawn fiber under applied tension of 0.3 MPa was heated by irradiating the CW CO_2 laser operated at 39.6 W cm^{-2}. The obtained microfiber has a diameter of about 1.8 μm and birefringence of 30×10^{-3}, and its draw ratio reaches a high value of 51,630. Until now, it has been impossible to attain such a high draw ratio with conventional drawing methods. Although the thinning process is induced by the plastic flow, the obtained microfiber was characterized by oriented crystallites and a high degree of the molecular orientation. The large deformation, attributed to the instantaneous plastic flow occurring from the molten state, causes strain-induced crystallization and molecular orientation. The thinning of the fiber by use of the laser may be conceived of as dieless spinning. Furthermore, we succeeded in winding the microfiber obtained by laser heating onto a spool. We will report these results in a future study.

The authors acknowledge the financial support of the Grant-in-Aid for Scientific Research (B) of Japan Society for the Promotion of Science.

References

1. Zergioti, I.; Hatziapostolou, A.; Hontzopoulos, E.; Zervaki, A.; Haidemenopoulos, G. N. Thin Solid Films 1995, 271, 96.
2. Wang, J.; Wong, W. C. K. J Mater Process Technol 1999, 95, 164.
3. Hopfe, V.; Jäckel, R.; Schönfeld, K. Appl Surf Sci 1996, 106, 60.
4. Paiva, P.; Madelino, F.; Conde, O. J Lumin 1999, 80, 141.
5. Panzner, M.; Wiedemann, G.; Henneberg, K.; Fischer, R.; Wittke, Th.; Dietsch, R. Appl Surf Sci 1998, 127–129, 787.
6. Hidouci, A.; Pelletier, J. M.; Ducoin, F.; Dezert, D.; El Guerjouma, R. Surf Coat Technol 2000, 123, 17.
7. Dadsetan, M.; Mirzadeh, H.; Shari, N. Radiat Phys Chem 1999, 56, 597.
8. Scarparo, M. A. F.; Chen, Q. J.; Miller, A. S.; Li, C. J.; Leary, H.; Allen, S. D. Appl Surf Sci 1996, 106, 275.
9. Suzuki, A.; Mochizuki, N. J Appl Polym Sci 2001, 82, 2775.
10. Suzuki, A.; Ishihara, M. J Appl Polym Sci 2002, 83, 1771.
11. Suzuki, A.; Mochizuki, N. J Appl Polym Sci 2003, 88, 3279.
12. Suzuki, A.; Mochizuki, N. J Appl Polym Sci 2003, 90, 1955.
13. Suzuki, A.; Kamata, K. J Appl Polym Sci Polym, to appear.
14. Natta, G.; Corradini, P. Nuovo Cimento Suppl 1960, 15, 40.
15. Natta, G. J Polym Sci 1955, 16, 143.
16. Kunugi, T.; Akiyama, I.; Hashimoto, M. Polymer 1982, 23, 1199.
17. Samuels, R. J. J Polym Part A 1965, 3, 1741.
18. Fujiwara, Y.; Goto, T.; Yamashita, Y. Polymer 1987, 28, 1253.
19. Tjong, S. C.; Shen, J. S.; Li, R. K. Y. Polymer 1996, 37, 2309.
20. Dorset, D. L.; McCourt, M. P.; Kopp, S.; Schumacher, M.; Okihara, T.; Lotz, B. Polymer 1998, 39, 6331.
21. Brücker, S.; Meille, S. V. Nature 1989, 340, 455.
22. Meille, S. V.; Brücker, S.; Porzio, W. Macromolecules 1990, 23, 4114.
23. Wills, A. J.; Capaccio, G.; Ward, I. M. J Polym Sci Polym Phys Ed 1980, 18, 493.
24. Hikosaka, M.; Seto, T. Polym J 1973, 5, 111.
25. Jacoby, P.; Bersted, B. H.; Kissel, W. J.; Smith, C. E. J Polym Sci Polym Phys Ed 1986, 24, 461.
26. Kalay, G.; Zhong, Z.; Allan, P.; Bevis, M. J. Polymer 1996, 37, 2077.
27. Napolitano, R. J Polym Sci Polym Phys Ed 1990, 28, 139.
28. Natta, G.; Corradini, P. Nuovo Cimento Suppl 1960, 15, 40.
29. Natta, G. J Polym Sci 1955, 16, 143.
30. Hsu, C. C.; Geil, P. H.; Miyaji, H.; Asai, K. J Polym Sci Polym Phys Ed 1986, 24, 2379.
31. Guerra, G.; Petraccone, V.; Corradini, P.; DeRosa, C.; Napolitano, R.; Pirozzi, B. J Polym Sci Polym Phys Ed 1984, 22, 1029.
32. Yadav, Y. S.; Jain, P. C. Polymer 1986, 27, 721.
33. Awaya, H. Polymer 1988, 29, 591.
34. Paukkeri, R.; Lehtinen, A. Polymer 1993, 34, 4075.
35. Paukkeri, R.; Lehtinen, A. Polymer 1993, 34, 4083.
36. Vleeshouwers, S. Polymer 1997, 38, 3213.